

Electrical properties of Ir/n-InGaN/Ti/Al Schottky barrier diode in a wide temperature range

R. Padma, V. Rajagopal Reddy*

Department of Physics, Sri Venkateswara University, Tirupati 517 502, India

*Corresponding author. Tel: (+91) 8772289472; E-mail: reddy_vrg@rediffmail.com

Received: 24 June 2013, Revised: 25 July 2013 and Accepted: 27 July 2013

ABSTRACT

The temperature dependent current-voltage (I-V) and capacitance-voltage (C-V) characteristics of Ir/n-InGaN Schottky contacts have been investigated and analysed in the temperature range of 100-400 K. The estimated barrier heights and ideality factor of Ir/n-InGaN Schottky diode are 0.30 eV (I-V), 1.15 eV (C-V) and 3.05 at 100 K, and 0.94 eV (I-V), 0.97 eV (C-V) and 1.20 at 400 K respectively. The barrier height (Φ_b), ideality factor (n) and series resistance (R_s) of Ir/n-InGaN Schottky diode are also evaluated using Cheung's and Norde methods. Results show that the barrier heights (I-V) increase while ideality factor and series resistance decrease with increasing temperature. Further, the discrepancy between Schottky barrier heights estimated from I-V and C-V measurements is also explained. It is observed that the interface state density N_{ss} decreases with an increasing temperature. Experimental results showed that the conduction current is dominated by Poole-Frenkel emission in the temperature range from 100 K to 340 K and by Schottky emission above 340 K. The dominate conduction mechanism changed from Poole-Frenkel to Schottky emission in the temperature range from 340 K to 370 K. Finally, it is concluded that the temperature-dependent $I-V$ characteristics of the Ir/n-InGaN Schottky diode can be successfully explained on the basis of thermionic emission (TE) mechanism. Copyright © 2014 VBRI press.

Keywords: Ir Schottky contact; n-type InGaN; Electrical characteristics; Schottky barrier heights; Series resistance; Poole-Frenkel and Schottky emissions.



R. Padma has obtained her M.Sc (Physics) from Sri Padmavathi Mahila Visvavidyalayam, Tirupati, India in 2007. Presently, she is working as project fellow in UGC-MRP project from 2011 at the Department of Physics, S.V.University, Tirupati. India. She has published four papers in refereed journals, and has been author more than two conference papers. Research interest is the fabrication and characterization of high quality Ohmic and Schottky contacts to III-V compound semiconductors.



V. Rajagopal Reddy received the M.Sc and Ph.D degrees in Physics from Sri Venkateswara University, Tirupati in 1989 and 1994. He is presently Professor in the Department of Physics, S.V.University, Tirupati. From September 2002 to December 2003, Prof. Reddy was a Visiting Research Professor, at the Semiconductor Thin Film and Device laboratory, Gwanju Institute of Science and Technology, Gwanju, Korea, where he performed research on Ohmic and Schottky Contacts to wide band gap semiconductors

(GaN). Prof. Reddy has published more than 125 articles in referred journals, and has been author or co-author of over 75 conference papers. His current research interests are (i) Ohmic and Schottky Contacts to wide-band gap semiconductors, (ii) Polymer-based Schottky Contacts to InP, (iii) Surface analysis of III-V and II-VI semiconductors, and (iv) Deep level studies in wide band gap semiconductors such as GaN, ZnO.

Introduction

Group III- nitride wide band gap semiconductors, particularly GaN and related alloys, are the most promising materials for the fabrication of electronic and optoelectronic devices due to their superior properties such as high breakdown field, good thermal conductivity, and high electron saturated velocity [1, 2]. Among the materials, ternary InGaN alloys with band gaps ranging from 0.7 to 3.4 eV which covering the entire visible spectrum are of interest for future optoelectronic and energy applications [3, 4]. Although, many works have been done on the optical characteristics of InGaN alloys, the electrical properties of this material are not being sufficiently investigated. The electrical characteristics and conduction mechanisms are the most important issues to realize the high quality Schottky devices. In order to fully understand the conduction current, the conduction mechanism should be investigated. However, only few investigations are made on the electrical properties and conduction mechanisms of metal/InGaN Schottky contacts. For example, Jang et al. [5] studied the Schottky barrier characteristics of Pt contacts to n-type InGaN. They found that the Schottky barrier heights (SBHs) determined by thermionic emission (TE) and thermionic field emission (TFE) modes using the (I-V) data are quite different from

each other. Jun et al. [6] studied the I-V characteristics of Au/Pt/InGaN/GaN heterostructure Schottky prototype solar cell and they reported that thermionic emission is a dominant current transport mechanism at the Pt/InGaN interface. Chen et al. [7] investigated the current transport mechanism of the Au/Pt/n-In_{0.2}Ga_{0.8}N Schottky contacts with different background carrier concentration. Shao et al. [8] studied the current transport mechanisms of InGaN metal-insulator-semiconductor (MIS) photodetectors with the two different insulating layers of Si₃N₄ and Al₂O₃. They reported that the space charge limit current (SCLC) is a dominant leakage conduction mechanism in the InGaN MIS photodetectors. They also noted that the SCLC mechanism is mediated by an exponential trap distribution and a bidirectional Fowler-Nordheim tunnelling effect is observed in the metal-Si₃N₄-InGaN photodetectors. Sang et al. [9] prepared thermally stable high performance InGaN MIS SPDs by using CaF₂ as the insulation layers. They studied reverse leakage current and UV responsivity at -3 V under 523 K without observing the persistent photoconductivity.

In our previous work, we have reported the detailed electrical, structural and morphological properties of the Ir/n-InGaN Schottky barrier diodes with different annealing temperatures [10, 11]. Analysis of the current-voltage (I-V) characteristics of the SBDs at room temperature only does not give detailed information about their conduction process or the nature of the barrier formed at the metal-semiconductor (M-S) interface. Therefore, in this work, a detailed analysis of the I-V and C-V characteristics Ir/n-InGaN Schottky contacts has been carried out in the temperature range 100 K-400 K to clarify the origin of the anomalous behavior of temperature dependence of the Schottky diode parameters such as the Schottky barrier height, ideality factor, series resistance (R_s) and interface state density (N_{ss}). Furthermore, the possible reverse current conduction mechanism of Ir/n-InGaN Schottky diode is described and discussed.

Experimental

Materials

2 μm-thick unintentionally doped GaN layer on a 40 nm-thick nucleation layer/ (0001) sapphire substrate was grown by metal organic chemical vapour deposition (MOCVD), followed by the growth of 0.25 μm-thick-n-InGaN:Si (N_d=7×10¹⁷ cm⁻³) with indium composition of 10%. Iridium (99.999%), Ti (99.999%) and Al (99.99%) metals were purchased from Sigma-Aldrich, India.

Methods

To remove contaminants, first the InGaN layer was initially degreased with organic solvents like trichloroethylene, acetone and methanol by means of ultrasonic agitation for 5 min in each step followed by rinsing in deionised (DI) water and then dried in N₂ flow. This degreased layer was then dipped into boiling aquarezia [HNO₃: HCl=1:3] for 10 min to remove the native oxide. The samples were directly loaded into the electron beam evaporation system, and a bilayer of Ti (25nm)/Al (100nm) was deposited to form ohmic contacts on InGaN. Then, the samples were annealed at 650°C for 1 min in flowing N₂ atmosphere using rapid thermal annealing (RTA) system. 50 nm thick

iridium (Ir) Schottky contacts of circular diameter of 0.7 mm through a stainless steel mask were fabricated on n-InGaN using electron beam evaporation system under vacuum pressure of 5×10⁻⁶ mbar.

The electrical characteristics were measured using a Keithly source measurement unit (Model No: 2400) and automated deep level transient spectrometer (SEMI LAB, DLS-83D). The current-voltage (I-V) and capacitance-voltage (C-V) characteristics were measured in the temperature range 100-400 K in steps of 30K in the dark. The device temperature is controlled with an accuracy of ± 1K by using temperature controller DLS-83D-1 cryostat.

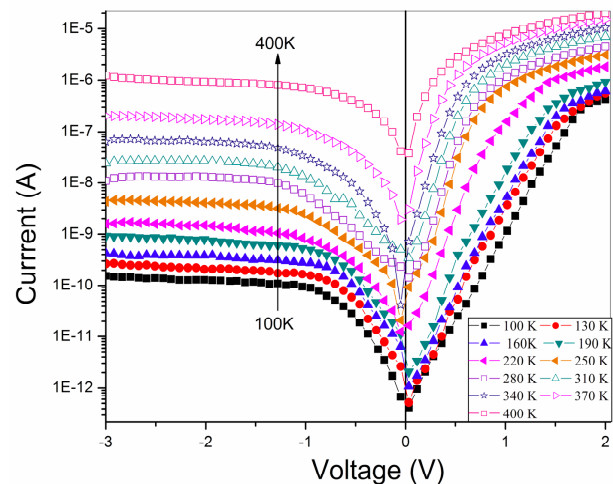


Fig. 1. Semi-logarithmic reverse and forward bias current-voltage characteristics of Ir/n-InGaN Schottky diode in the temperature range of 100-400 K in steps of 30 K.

Results and discussion

Fig. 1 shows the semi-logarithmic plot of forward and reverse I-V characteristics of Ir/n-InGaN Schottky barrier diode (SBD) in the temperature range of 100-400K in steps of 30K. Total twelve Ir/n-InGaN Schottky diodes are fabricated. In all the cases, similar I-V and C-V characteristics are observed. Only one Schottky diode is used for temperature-dependent characteristics. The observed leakage current for Ir/n-InGaN Schottky diode is 2.22×10^{-11} A for 100 K to 7.64×10^{-7} A for 400 K at -1V, respectively. It is noted that the leakage current decreases with decrease in temperature as well as consisted Schottky barrier height inhomogeneity. Probably, the origin of leakage current is due to deep level impurity or edge leakage currents [12, 13]. We analyze the experimental I-V curves according to thermionic theory (TE) in which the current-voltage characteristics are given by the relation [14-17].

$$I = I_o \exp\left(\frac{qV}{nkT}\right) \left[1 - \exp\left(\frac{-qV}{kT}\right) \right] \quad (1)$$

$$\text{with } I_o = AA^{**} T^2 \exp\left(\frac{-q\Phi_b}{kT}\right) \quad (2)$$

Here I_0 is the saturation current, q is the electron charge, V is the applied voltage, T is the absolute temperature, n is the ideality factor, k is the Boltzman's constant, A is the contact area, A^{**} is the effective Richardson's constant ($23 \text{ A cm}^{-2} \text{ K}^{-2}$ for n-InGaN based on the effective mass ($m^*=0.19 m_0$)) [5], and Φ_b is the Schottky barrier height (SBH). The saturation current I_0 derived from the plot $\ln I/[1-\exp(-qV/kT)]$ versus V (figure is not shown here) is a straight line and intercepts the current axis at $V=0$ using experimental data from which the SBH is defined in terms of TE and is given by

$$\Phi_b = \frac{kT}{q} \ln\left(\frac{AA^*T^2}{I_0}\right) \quad (3)$$

The ideality factor 'n' can be determined from the slope of the linear region of the forward bias $\ln I$ versus V plot, and measure the conformity of the diode due to pure TE. This can be written as

$$n = \frac{q}{kT} \left(\frac{dV}{d(\ln I)} \right) \quad (4)$$

The value of the barrier heights Φ_b and ideality factors (n) of the Ir/n-InGaN Schottky diode at different temperatures are calculated using the equation (3) and (4) and values are given in **Table 1**.

Table 1. The various parameters calculated from I-V and C-V measurements of Ir/n-InGaN Schottky diode as a function of temperature.

Temp. (K)	Schottky barrier height Φ_b (eV)		Ideality factor From I-V	Cheung's functions		Norde		Interface State density		
	I-V	C-V		n	R_s (Ω)	n	Φ_b (eV)	R_s (Ω)	Φ_b (eV)	R_s (Ω)
100	0.30	1.15	3.05	1010	4.90	0.33	1185	0.40	1358	4.27×10^{13}
130	0.39	1.13	2.78	937	4.58	0.40	986	0.48	1103	3.70×10^{13}
160	0.48	1.12	2.56	720	4.10	0.49	751	0.57	956	3.24×10^{13}
190	0.58	1.11	2.21	515	3.91	0.60	568	0.66	789	2.50×10^{13}
220	0.64	1.10	2.05	470	3.48	0.65	489	0.71	690	2.16×10^{13}
250	0.73	1.07	1.93	310	3.01	0.74	362	0.76	622	1.90×10^{13}
280	0.80	1.06	1.84	285	2.95	0.81	311	0.83	552	1.71×10^{13}
310	0.85	1.03	1.72	231	2.80	0.86	267	0.89	384	1.46×10^{13}
340	0.90	1.00	1.55	184	2.45	0.91	214	0.92	316	1.10×10^{13}
370	0.92	0.98	1.31	133	1.95	0.93	159	0.93	258	5.91×10^{12}
400	0.94	0.97	1.20	105	1.60	0.96	116	0.94	189	3.56×10^{12}

The calculated Schottky barrier height increases from 0.30 eV at 100 K to 0.94 eV at 400 K and the ideality factor decreases from 3.05 at 100 K to 1.20 at 400 K. Interestingly, it is noted that the SBH is found to increase with temperature whereas the ideality factor (n) is found to decrease with temperature. As explained in the literature [18-20], since the current transport across the metal/semiconductor (MS) interface is a temperature activated process, electrons at low temperature are able to surmount the lower barriers and therefore the current transport will be dominated by the current flowing through the patches of lower SBH and a large ideality factor. As the temperature increases, more and more electrons have sufficient energy to surmount the higher barrier. As a

result, the dominant barrier height will increase with temperature. An apparent increase in the ideality factor and a decrease in the barrier height at low temperatures are caused possibly by other effects such as inhomogeneities of thickness and non-uniformity of the interfacial charges.

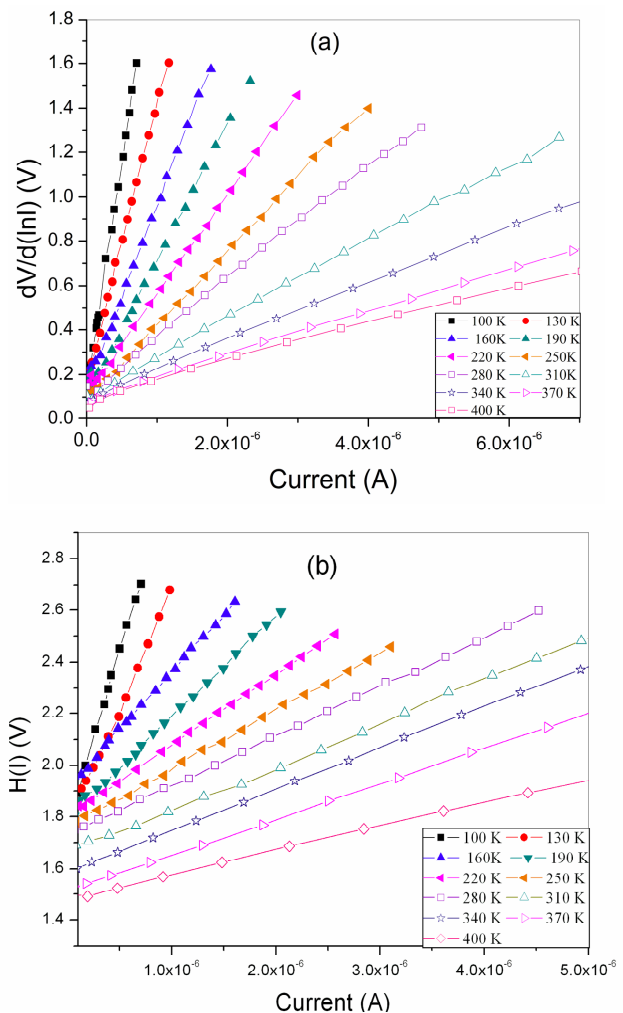


Fig. 2. (A) Plot of $dV/d(\ln I)$ versus I for Ir/n-InGaN Schottky diode in the temperature range of 100-400K, (B) Plot of $H(I)$ versus I for the Ir/n-InGaN Schottky diode in the temperature range of 100-400 K.

As can be seen from **Fig. 1**, at low bias voltage the semi-logarithmic forward bias I-V characteristics are linear, but at high voltage deviated from linearity due to R_s effect. Therefore R_s is a very important parameter and it deviate barrier height and ideality factor significantly at low temperatures from accuracy of determination. The current-voltage characteristics of Ir/n-InGaN Schottky contact show rectification behaviour. Here, from the forward bias I-V data the barrier height, ideality factor and series resistance can be estimated using a method developed by Cheung and Cheung [21]. Cheung's functions can be expressed as follows;

$$\frac{dV}{d(\ln I)} = IR_s + n \left(\frac{kT}{q} \right) \quad (5)$$

$$H(I) = V - n \left(\frac{kT}{q} \right) \ln \left(\frac{I}{AA^{**}T^2} \right) \quad (6)$$

and

$$H(I) = IR_s + n\Phi_b \quad (7)$$

Experimental $dV/d\ln(I)$ versus I and $H(I)$ versus I plots at different temperatures for Ir/n-InGaN Schottky diode are shown in **Fig. 2 (A)** and **(B)**. Equation (5) should give a straight line for the data of downward curvature in the forward bias I-V characteristics. Thus, a plot of $dV/d\ln(I)$ versus I will give the $n(kT/q)$ as the y-intercept and R_s as the slope. The series resistance and ideality factor of the Ir/n-InGaN Schottky diode are found to be 1010 Ω and 4.90 at 100 K and 105 Ω and 1.60 at 400 K. Using the n value determined by the $dV/d\ln(I)$ versus I plot, a plot of $H(I)$ versus I also will give a straight line with a y-intercept equal to $n\Phi_b$. The slope of these plots also provides a second determination of R_s which can be used to check the consistency of Cheung's method. The barrier height and series resistance estimated from the plot of $H(I)$ versus I are found to be 0.33 eV and 1185 Ω at 100 K, and 0.96 eV and 116 Ω at 400 K. The ideality factor values obtained from the downward curvature regions of forward bias I-V plots and from the linear regions of the same characteristics are different from each other. This may be due to the effects such as bias dependence of SBH according to the voltage drop across the interfacial layer and the change of the interface states with the bias in the low-voltage region of the current-voltage plot and the series resistance.

In order to determine the values of the SBH and series resistance of Ir/n-InGaN Schottky barrier diode, Norde proposed an empirical function. The modified Norde function is defined as [22].

$$F(V) = \frac{V}{\gamma} - \frac{1}{\beta} \ln \left[\frac{I(V)}{AA^{**}T^2} \right] \quad (8)$$

where γ is an integer (dimensionless) greater than the ideality factor, $I(V)$ is the current obtained from the I-V curve, and β is a temperature dependent value calculated using $\beta = q/kT$. The effective SBH is given by

$$\Phi_b = F(V_o) + \frac{V_o - kT}{\gamma q} \quad (9)$$

where $F(V_o)$ is the minimum point of $F(V)$ and V_o is the corresponding voltage. A plot of the Norde function $F(V)$ versus V for the Ir/n-InGaN Schottky barrier diode is shown in **Fig. 3**.

The value of series resistance (R_s) can be determined from the Norde function is

$$R_s = \frac{kT(\gamma - n)}{qI} \quad (10)$$

Where, I is the current in the device corresponding to voltage V_{min} (at which $F(V)$ becomes minimum). From the Norde plot, the barrier height and the series resistance values are found to be 0.40eV, 1358 Ω at 100 K and 0.94 eV, 189 Ω at 400 K respectively.

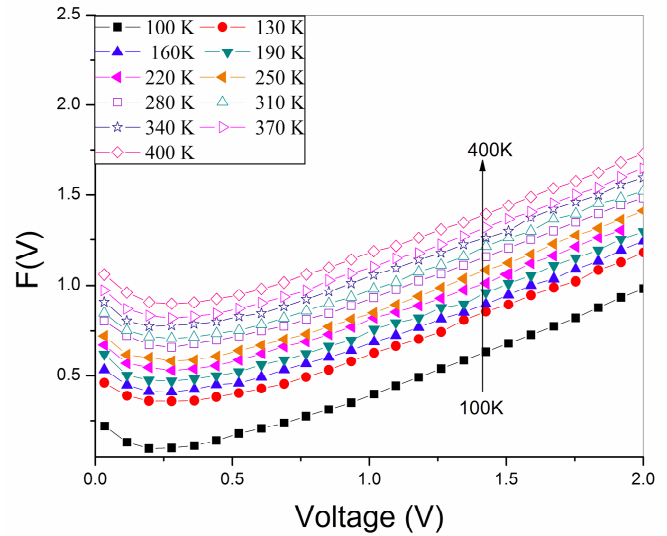


Fig. 3. Plot of $F(V)$ versus V for Ir/n-InGaN Schottky diode in the temperature range of 100-400 K.

The values of barrier height obtained from the Norde function are in good agreement with the values obtained from I-V characteristics (**Fig. 1**) and Cheung's functions (**Fig. 2(B)**). **Fig. 4** shows the experimental series resistance values from the semi-log forward bias I-V characteristics as a function of temperature.

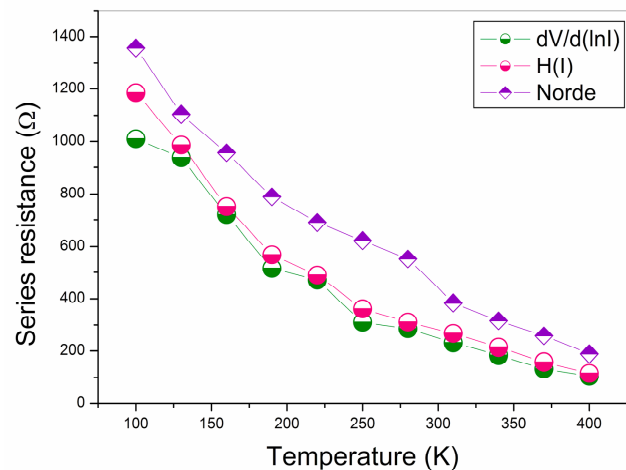


Fig. 4. Plot of series resistance with temperature obtained by Cheung's method and Norde method for Ir/n-InGaN Schottky diode.

The values of series resistance from the plots of $dV/d\ln(I)$ versus I are identical to those from the plot of $H(I)$ versus I . On the other hand, the value of series resistance obtained from Norde function is slightly higher than that obtained from Cheung functions. Cheung functions are only applied to the non-linear region in high voltage region of the forward-bias $\ln I$ -V characteristics, while Norde's functions are applied to the full forward-bias region of the $\ln I$ -V characteristics of the diodes. The series resistance R_s

obtained using different methods for each temperature of the I-V data decreases with increase of temperature. The decrease of R_s with the rise of temperature may be due to factors responsible for increase in the ideality factor 'n' and lack of free carrier concentration at low temperature [23,24].

Fig. 5 shows C^{-2} -V plots of Ir/n-InGaN Schottky barrier diode at the frequency of 1 MHz with an ac modulation of 100 mV in the dark.

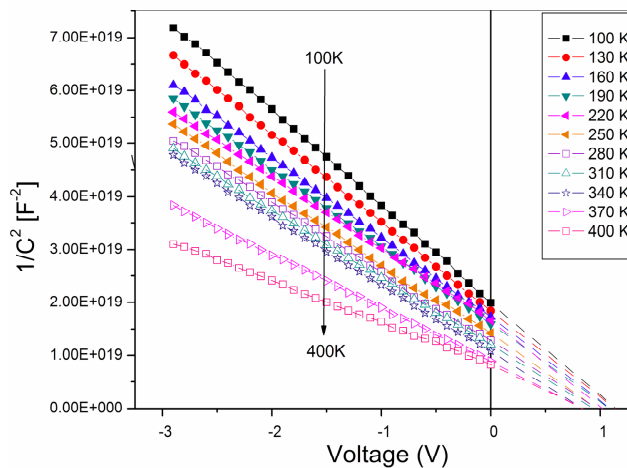


Fig. 5. The reverse bias C^{-2} -V characteristics of the Ir/n-InGaN Schottky diode in the temperature range of 100-400 K.

The C-V relationship for Schottky diode is given by [25]

$$\frac{1}{C^2} = \left(\frac{2}{\epsilon_s q N_d A^2} \right) \left(V_{bi} - \frac{kT}{q} - V \right) \quad (11)$$

where ϵ_s is the permittivity of the semiconductor $\epsilon_s = 8.4 \epsilon_0$, V is the applied voltage, q is the electronic charge, N_d is the donor concentration, A is the area of the Schottky contact and V_{bi} is the flat band voltage. The x-intercept of the plot of $(1/C^2)$ versus V gives V_0 and it is related to the built in potential V_{bi} by the equation $V_{bi} = V_0 + kT/q$, where T is the absolute temperature. The barrier height $\Phi_{b(C-V)}$ is given by the equation $\Phi_{b(C-V)} = V_0 + V_n + kT/q$, here $V_n = (kT/q) \ln(N_c/N_d)$. The density of the states in the conduction band edge is given by $N_c = 2(2\pi m^* kT/h^2)^{3/2}$, where $m^* = 0.19 m_0$ [5]. The calculated barrier heights of Ir/n-InGaN are in the range of 1.15 eV (for 100K) to 0.97 eV (for 400K). As can be seen from Fig. 6, it is noted that the measured barrier height values by the I-V method are lower than those calculated by the C-V method. The differences in barrier height values estimated from the I-V and C-V methods may be due to the presence of an insulating layer or charges existing at the metal-semiconductor interface, deep impurity levels, image force barrier lowering, and edge leakage currents [14, 16, 26]. Another explanation for the discrepancy between measured I-V and C-V barrier heights could be associated with the barrier height inhomogeneity at the interface. The barrier height obtained from the I-V technique is logically low or a combination of low and high, known as parallel contacts, as the I-V method involves the flow of electrons from the semiconductor to the metal [27, 28]. Otherwise, the C-V

measured barrier height influenced by the distribution of charge at the depletion region boundary and this charge distribution follows the weighted arithmetic average of the SBHs. According to Werner and Guttler [18], any spatial discrepancy in the barriers causes the current to flow preferentially through the barrier minima. Clearly, the current is dominated in the I-V data by the current which flows through the region of low SBH [29].

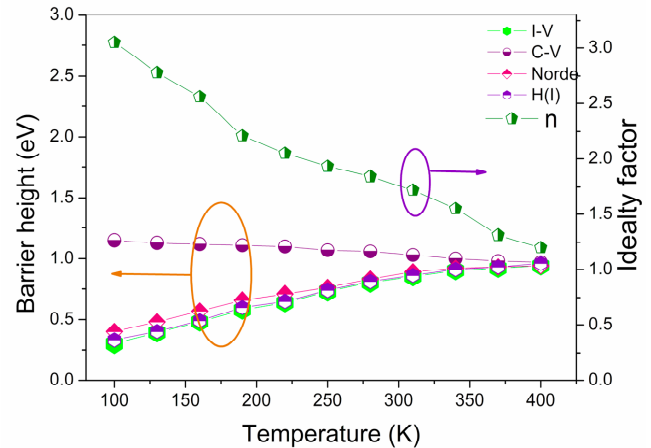


Fig. 6. The comparison of barrier heights and ideality factor of Ir/n-InGaN Schottky diode with temperatures ranging from 100 to 400 K.

Geng et al. [30] reported that the pinholes come from the extended coreless dislocations, which were originating in the GaN buffer layer. A large number of dislocations or pinholes spread in a sample, resulting in a high leakage current and low BH. However, much less dislocations or pinholes appear on the surface of sample results in low leakage current and high effective BH. Generally, C-V measurements are less prone to dislocations or pinholes, so that the determined BH is considered more reliable, though the depletion width can be altered by the interface defects if they are deeper into the space charge region.

For a Schottky diode having interface states in equilibrium with the semiconductor, the ideality factor becomes greater than unity as proposed by Card and Rhoderick [31] and is given by;

$$n(V) = 1 + \frac{\delta}{\epsilon_i} \left[\frac{\epsilon_s}{W_d} + qN_{SS}(V) \right] \quad (12)$$

where W_d is the space charge width, N_{SS} is the density of interface states, ϵ_s and ϵ_i are the permittivity of the semiconductor and the interfacial layer, respectively. The voltage dependent ideality factor $n(V)$ can be expressed as $n(V) = V/(kT/q) \ln(I/I_s)$. According to equation (12), the interface state density can be written as;

$$N_{SS} = \frac{1}{q} \left[\frac{\epsilon_i}{\delta} (n(V) - 1) - \frac{\epsilon_s}{W_d} \right] \quad (13)$$

In the n-type semiconductor, the energy of the interface states E_{SS} with respect to the bottom of the conduction band at the surface of the semiconductor is given by [32];

$$E_C - E_{SS} = q(\Phi_e - V) \quad (14)$$

where Φ_e is the effective barrier height. The voltage dependence of the effective barrier height Φ_e is contained in the ideality factor, n through the relation;

$$\frac{d\Phi_e}{dv} = \beta = 1 - \frac{1}{n(V)} \quad (15)$$

where β is the voltage coefficient of Φ_e . The effective barrier height Φ_e is given by

$$\Phi_e = \Phi_b + \beta(V) \quad (16)$$

The values of N_{SS} as a function of V are obtained and are given in **Table 1**. The resulting dependence of N_{SS} is converted to a function of E_{SS} using equation (14). **Fig. 7** shows the plot of N_{SS} versus $E_C - E_{SS}$ at different temperatures. From **Fig. 7**, it is seen an exponential increase in the N_{SS} from midgap towards the bottom of the conduction band.

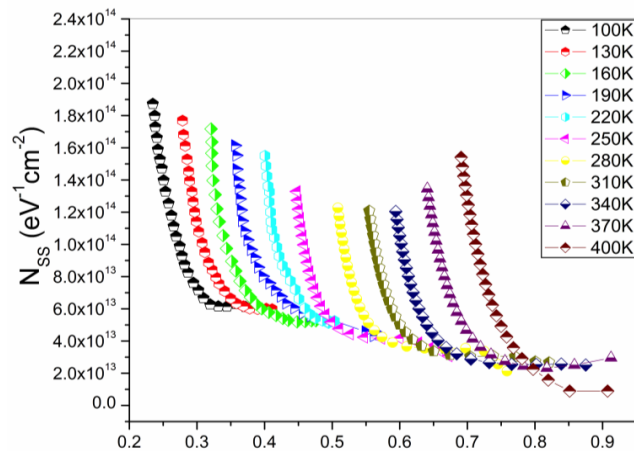


Fig. 7. A plot of N_{SS} versus $E_C - E_{SS}$ for Ir/n-InGaN Schottky diode with temperatures ranging from 100 to 400 K.

The interface state density as calculated using Terman's method [33] varies from $4.27 \times 10^{13} \text{ eV}^{-1} \text{ cm}^{-2}$ at 100 K to $3.56 \times 10^{12} \text{ eV}^{-1} \text{ cm}^{-2}$ at 400 K. It is noted that the dependency of the interface state density (N_{SS}) on the measurement temperature. Decreasing of N_{SS} with an increasing temperature can be explained with the variation of the ideality factor as a function of temperature due to lateral inhomogeneities of the barrier height at the metal-semiconductor interface [34]. According to Akkal [35], the decrease of N_{SS} with an increase in the temperature may also be due to molecular restructuring and reordering of the metal/semiconductor interface under the effect of temperature.

The reverse I-V characteristics give further information on the conduction mechanism of Ir/n-InGaN Schottky barrier diodes. The field-dependent effects are more pronounced at reverse biases because of larger electrical fields involved in this bias. Usually, the carrier

recombination in the depletion layer and image force lowering of the barrier height often dominates the reverse characteristics of Schottky diodes since the reverse bias increases the electric field in the junction. The current transport mechanism dominating the reverse leakage current in the Ir/n-InGaN Schottky diode is investigated using the electric field dependence considering by Poole-Frenkel and Schottky emission across the junction. The current through the diode when dominated by Poole-Frenkel effect is given by [36-38]

$$I_R = I_o \exp\left(\frac{\beta_{PF}}{K_B T} \sqrt{E}\right) \quad (17)$$

For the Schottky effect,

$$I_R = AA^* T^2 \exp\left(\frac{\beta_S}{K_B T} \sqrt{E}\right) \quad (18)$$

where β_{PF} and β_S are the Poole-Frenkel and Schottky field-lowering coefficients, respectively. The theoretical values for β_{PF} and β_S are given by

$$2\beta_S = \beta_{PF} = \left(\frac{q^3}{\pi\epsilon}\right)^{1/2} \quad (19)$$

In principle the Poole-Frenkel and Schottky effects can be distinguished by the measured values of field-lowering coefficients. The Poole-Frenkel field-lowering coefficient (β_{PF}) is always twice the value of the Schottky field-lowering coefficients (β_S). The theoretical values of field-lowering coefficients β_{PF} and β_S for the Ir/n-InGaN Schottky diode obtained from equation (19) are $\beta_{PF} = 2.62 \times 10^{-5} \text{ eV/m}^{1/2} \text{ V}^{-1/2}$ and $\beta_S = 1.31 \times 10^{-5} \text{ eV/m}^{1/2} \text{ V}^{-1/2}$.

Fig. 8 shows a plot of $\ln(I_R)$ versus $E^{1/2}$ for Ir/n-InGaN Schottky diode at different temperatures.

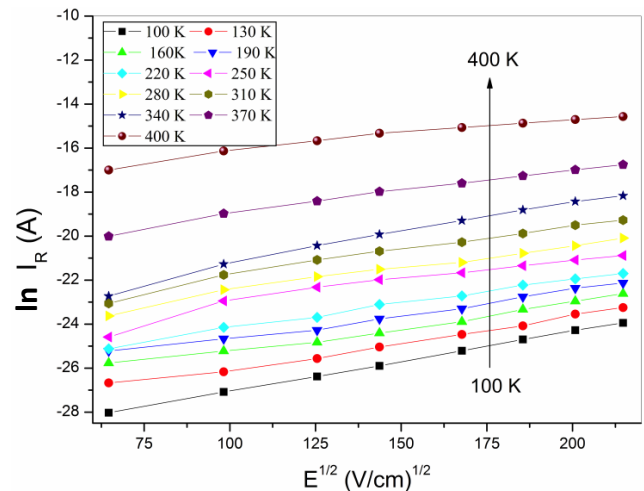


Fig. 8. A plot of $\ln(I_R)$ versus $E^{1/2}$ for Ir/n-InGaN Schottky diode at temperatures ranging from 100 to 400 K.

For Ir/n-InGaN Schottky diode, the experimental slopes determined from the fit to the data are $2.99 \times 10^{-5} \text{ eV/m}^{1/2} \text{V}^{-1/2}$ for 100 K, 2.95×10^{-5} , 2.87×10^{-5} , 2.78×10^{-5} , 2.72×10^{-5} , 2.70×10^{-5} , 2.61×10^{-5} , 2.51×10^{-5} , 2.47×10^{-5} for 130, 160, 190, 220, 250, 280, 310 and 340 K, and 1.67×10^{-5} , $1.44 \times 10^{-5} \text{ eV/m}^{1/2} \text{V}^{-1/2}$ for 370 K and 400 K respectively. The experimental slope values of the Ir/n-InGaN Schottky diode are closely matched to the theoretical slopes of the Poole-Frenkel mechanism in the temperature range of 100-340 K and Schottky emission in the temperature range of 370-400 K. A comparison of the experimental and theoretical slopes revealed that the experimental slopes obtained in the low temperature region ($T \leq 340 \text{ K}$) are closer to the Poole-Frenkel field-lowering coefficient (β_{PF}). While the experimental slopes in the higher temperature region ($T \geq 370 \text{ K}$) are closer to the Schottky field-lowering coefficient (β_{S}). This suggests that the leakage current is found to be dominated by Poole-Frenkel emission in the lower temperature region ($T < 340 \text{ K}$) whereas Schottky emission is dominant in the higher temperature region ($T > 370 \text{ K}$). It is noted that the conduction mechanism of Ir/n-InGaN/Ti/Al Schottky diode changed from Poole-Frenkel emission to Schottky emission in the temperature range from 340 to 370 K.

Conclusion

In conclusion, the electrical properties of Ir/n-InGaN Schottky barrier diodes have been investigated in the temperature range of 100–400K. The calculated SBHs from I-V measurements are in the range of 0.30 at 100 K to 0.94 eV at 400 K with the ideality factor of 3.05 at 100 K to 1.20 at 400 K. It is noted that the SBH increases whereas ideality factor decreases with increasing temperature. The barrier heights calculated from C-V measurements decreases with increase in temperature and values are in the range of 1.15 eV to 0.97 eV at 100 to 400 K. Using Norde and Cheung functions, the barrier height (Φ_{b}), ideality factor (n) and series resistance (R_{s}) are also calculated and these values are found to be strongly temperature dependent. It is noted that there are reasonably good agreement among the values of barrier height obtained from the forward-bias I-V characteristics, Norde and Cheung functions. The interface state density N_{SS} is determined from the I-V and C-V data using Terman's method for Ir/n-InGaN Schottky diode in the temperature range of 100-400 K. It is found to be decreased with an increasing temperature. At 100-340 K, Poole-Frenkel emission is found to be responsible for the reverse leakage current, whereas Schottky emission is the dominant mechanism at high temperatures (370-400 K). There is a transition of the conduction mechanism from Poole-Frenkel to Schottky emission at 340–370 K.

Acknowledgements

The authors thank the University Grant Commission (UGC), New Delhi, India for providing the financial assistance (Grant no. 39-530/2010 (SR)).

Reference

- Khan, M.A.; Bhattarai, A.; Kuznia, J.N.; Olson, D.T.; *Appl. Phys. Lett.* **1993**, *63*, 1214.
DOI: [10.1063/1.109775](https://doi.org/10.1063/1.109775)
- Nakamura, S.; Senoh, M.; Nagahama, S.; Iwasa, N.; Yamada, T.; Matsushita, T.; Sugimoto, Y.; Kiyoku, H.; *Appl. Phys. Lett.* **1996**, *69*, 4056.
DOI: [10.1063/1.109775](https://doi.org/10.1063/1.109775)
- Nakamura, S.; Fasol, G.; *The blue laser diode*, Springer, Berlin, **1997**.
- Gil, B.; *Ground III Nitride Semiconductor Compounds: Physics and applications*, Oxford, New York, **1998**.
- Jang, J.-S.; Kim, D.; Seong, T.-Y.; *J. Appl. Phys.* **2006**, *99*, 073704.
DOI: [10.1063/1.2187274](https://doi.org/10.1063/1.2187274)
- Jun-Jun, X.; Dun-Jun, C.; Bin, L.; Zin-Li, X.; Ruo-Lian, J.; Rong, Z.; You-Dou, Z.; *Chin. Phys. Lett.* **2009**, *26*, 098102.
DOI: [10.1088/0256-307X/26/9/098102](https://doi.org/10.1088/0256-307X/26/9/098102)
- Chen, D.J.; Huang, Y.; Liu, B.; Xie, Z.L.; Zhang, R.; Zheng, Y.D.; Wei, Y.; Narayanamurti, V.; *J. Appl. Phys.* **2009**, *105*, 063714.
DOI: [10.1063/1.3099601](https://doi.org/10.1063/1.3099601)
- Shao, Z.G.; Chen, D.J.; Liu, B.; Lu, H.; Xie, Z.L.; Zhang, R.; Zheng, Y.D.; *J. Vac. Sic. Technol. B* **2011**, *29*, 1017.
DOI: [10.1116/1.3622298](https://doi.org/10.1116/1.3622298)
- Sang, L.; Liao, M.; Koide, Y.; Sumiya, M.; *Appl. Phys. Lett.* **2011**, *98*, 103502.
DOI: [10.1063/1.3562326](https://doi.org/10.1063/1.3562326)
- Rajagopal Reddy, V.; Prasanna Lakshmi, B.; Padma, R.; *J. Metallurgy* **2012**, *2012*, 1.
DOI: [10.1155/2012/531915](https://doi.org/10.1155/2012/531915)
- Rajagopal Reddy, V.; Padma, R.; Siva Pratap Reddy, M.; Choi, C.-J.; *Phys. Stat. Solidi A* **2012**, *209*, 2027.
DOI: [10.1002/pssa.201228224](https://doi.org/10.1002/pssa.201228224)
- Zhang, H.; Miller, E.J.; Yu, E.T.; *Appl. Phys. Lett.* **2006**, *99*, 023703.
DOI: [10.1063/1.2159547](https://doi.org/10.1063/1.2159547)
- Hsu, J.W.P.; Manfra, M.J.; Molnar, R.J.; Heying, B.; Speck, J.S.; *Appl. Phys. Lett.* **2002**, *81*, 79.
DOI: [10.1063/1.1490147](https://doi.org/10.1063/1.1490147)
- Rhoderick, E.H.; Williams, R.H.; *Metal-Semiconductor Contacts*, Clarendon, Oxford, **1998**.
- Henisch, H.K.; *Semiconductor contacts*, Oxford, London, **1984**.
- Tung, R.T.; *Mater. Sci. Eng. R* **2001**, *35*, 1.
DOI: [10.1016/S0927-796X\(01\)00037-7](https://doi.org/10.1016/S0927-796X(01)00037-7)
- Wilmsen, C.W.; Williams, R.H.; Robison, G.Y.; *Physics and Chemistry of III-V Compound Semiconductor Interfaces*, Plenum, New York, **1985**.
- Wernner, J.H.; Guttler, H.H.; *J. Appl. Phys.* **1991**, *69*, 1522.
DOI: [10.1063/1.347243](https://doi.org/10.1063/1.347243)
- Wernner, J.H.; Guttler, H.H.; *J. Appl. Phys.* **1993**, *73*, 1315.
DOI: [10.1063/1.353249](https://doi.org/10.1063/1.353249)
- Sullivan, J.P.; Tung, R.T.; Pinto, M.R.; Graham, W.R.; *J. Appl. Phys.* **1991**, *70*, 7403.
DOI: [10.1063/1.349737](https://doi.org/10.1063/1.349737)
- Cheung, S.K.; Cheung, N.W.; *Appl. Phys. Lett.* **1980**, *49*, 85.
DOI: [10.1063/1.97359](https://doi.org/10.1063/1.97359)
- Norde, H.; *J. Appl. Phys.* **1979**, *50*, 5052.
DOI: [10.1063/1.325607](https://doi.org/10.1063/1.325607)
- Chand, S.; Kumar, J.; *J. Appl. Phys.* **1996**, *80*, 288.
DOI: [10.1063/1.362818](https://doi.org/10.1063/1.362818)
- Chand, S.; Kumar, J.; *Appl. Phys. A* **1996**, *63*, 171.
DOI: [10.1007/BF01567648](https://doi.org/10.1007/BF01567648)
- Eftekhari, G.; *J. Vac. Sci. Technol. B* **1993**, *11*, 1317.
DOI: [10.1116/1.586936](https://doi.org/10.1116/1.586936)
- Hacke, P.; Detchprohm, T.; Hiramatsu, K.; Sawaki, N.; *Appl. Phys. Lett.* **1993**, *63*, 2676.
DOI: [10.1063/1.110417](https://doi.org/10.1063/1.110417)
- Ohdomari, I.; Tu, K.N.; *J. Appl. Phys.* **1980**, *51*, 3735.
DOI: [10.1063/1.328160](https://doi.org/10.1063/1.328160)
- Freeouf, J.L.; Jackson, T.N.; Laux, S.E.; Woodall, J.M.; *Appl. Phys. Lett.* **1982**, *40*, 634.
DOI: [10.1063/1.93171](https://doi.org/10.1063/1.93171)
- Shivaraman, S.; Herman, L.H.; Rana, F.; Park, J.; Spencer, M.G.; *Appl. Phys. Lett.* **2012**, *100*, 183112.
DOI: [10.1063/1.4711769](https://doi.org/10.1063/1.4711769)
- Geng, L.; Ponce, F.A.; Tanaka, S.; Omiya, H.; Nakagawa, Y.; *Phys. Stat. Sol. A* **2001**, *188*, 803.
DOI: [10.1002/1521-396X\(200112\)188:2<803](https://doi.org/10.1002/1521-396X(200112)188:2<803)
- Card, H.C.; Rhoderick, E.H. *J. Phys. D: Appl. Phys.* **1971**, *4*, 1589.
DOI: [10.1088/0022-3727/4/10/319](https://doi.org/10.1088/0022-3727/4/10/319)
- Hudiat, M.K.; Krupanidhi, S.B.; *Mater. Sci. Eng. B* **2001**, *87*, 141.
DOI: [10.1016/S0921-5107\(01\)00713-9](https://doi.org/10.1016/S0921-5107(01)00713-9)
- L.M. Terman, *Solid-State Electron.* **1962**, *5*, 285.
DOI: [10.1016/S0038-1101\(62\)90111-9](https://doi.org/10.1016/S0038-1101(62)90111-9)

34. P. Cova, A. Sing, A. Medina, R.M. Masut, *Solid-State Electron.* **1997**, 42, 477.
DOI: [10.1016/S0038-1101\(97\)00250-5](https://doi.org/10.1016/S0038-1101(97)00250-5)
35. Akkal, B.; Benemara, Z.; Boudissa, A.; Bouiadjra, N.B.; Amrani, M.; Bideux, I. *Mater. Sci. Eng. B* **1998**, 55, 162.
DOI: [10.1016/S0921-5107\(98\)00168-8](https://doi.org/10.1016/S0921-5107(98)00168-8)
36. Schottky, W. Z.; *Physik* **1914**, 15, 872.
DOI: [10.1106/Physik.15.872](https://doi.org/10.1106/Physik.15.872)
37. Frenkel, J.; *Phys. Rev.* **1938**, 54, 647.
DOI: [10.1103/PhysRev.54.647](https://doi.org/10.1103/PhysRev.54.647)
38. Mead, C.A.; *Phys. Rev.* **1962**, 128, 2088.
DOI: [10.1103/PhysRev.128.2088](https://doi.org/10.1103/PhysRev.128.2088)

Advanced Materials Letters

Publish your article in this journal

[ADVANCED MATERIALS Letters](#) is an international journal published quarterly. The journal is intended to provide top-quality peer-reviewed research papers in the fascinating field of materials science particularly in the area of structure, synthesis and processing, characterization, advanced-state properties, and applications of materials. All articles are indexed on various databases including [DOAJ](#) and are available for download for free. The manuscript management system is completely electronic and has fast and fair peer-review process. The journal includes review articles, research articles, notes, letter to editor and short communications.

